

# Lithography-free plasmonic color printing with femtosecond laser on semicontinuous silver films

*Sarah N. Chowdhury<sup>1\*</sup>, Piotr Nyga<sup>1,2\*</sup>, Zhaxylyk A. Kudyshev<sup>1</sup>, Esteban Garcia Bravo<sup>3</sup>,  
Alexei S. Lagutchev<sup>1</sup>, Alexander V. Kildishev<sup>1</sup>, Vladimir M. Shalaev<sup>1</sup>,  
and Alexandra Boltasseva<sup>1</sup>*

1. School of Electrical and Computer Engineering and Birck Nanotechnology Center, Purdue University, 1205 W State St, West Lafayette IN, 47907, USA

2. Institute of Optoelectronics, Military University of Technology, 2 Kaliskiego St, Warsaw, 00-908, Poland

3. Department of Computer Graphics Technology, Purdue University, 401 N. Grant St, Knott Hall, West Lafayette, IN 47907, USA

\* equal contribution

**KEYWORDS.** Plasmonics; plasmonic color, semicontinuous metal films; color printing; laser modifications.

## **ABSTRACT**

Plasmonic color printing with semicontinuous metal films is a lithography-free, non-fading, and environment-friendly method of generation of bright colors. Such films are comprised of metal nanoparticles, which resonate at different wavelengths upon light illumination depending on the size and shape of the nanoparticles. To achieve an experimentally demonstrated structure

that was optimized in terms of broader color range and increased stability, variable Ag semicontinuous metal films were deposited on a metallic mirror with a sub-wavelength-thick dielectric spacer. Femtosecond laser post-processing was then introduced to extend the color gamut through spectrally induced changes from blue to green, red, and yellow. Long-term stability and durability of the structures were addressed to enable non-fading colors with an optimized overcoating dielectric layer. The thickness of the proposed designs is on the order of 100 nanometers, and it can be deposited on any substrate. These structures generate a broad range of long-lasting colors in reflection that can be applied to real-life artistic or technological applications with a spatial resolution on the order of 0.3 mm or less.

## INTRODUCTION

We currently have about sixteen million colors available in the realm of natural and artificial palette<sup>1</sup>, and still, everyday people are yearning for new shades of color. Unfortunately, this full- color range of mostly synthetic (artificial) dyes expels toxic chemicals that are not non-biodegradable and carcinogenic,<sup>2</sup> and are capable of altering the physical and chemical properties of soil, deteriorating water bodies, and causing irreversible harm to flora and fauna.<sup>3</sup> Coloration using plasmonic nanostructures has been in vogue for centuries,<sup>4,5</sup> but recently it has been used for sub-wavelength printing.<sup>6–20</sup> Exemplary work on color generation using plasmonic structures has been done with sub-wavelength resolution e-beam lithography<sup>8,14,16–18,20,21</sup> and ion milling<sup>7,13,15,19</sup> but the fabrication cost impedes the scalable reproduction of plasmonic color fine art and technological samples.

Semicontinuous metal films (SMF), which are disordered films made of metallic nanoparticles, have been recently explored for plasmonic coloration<sup>22–24</sup>. Such films can be achieved at the initial stage of the deposition of a metallic layer on a planar substrate, where instead of a continuous film, metal nanoparticles of different sizes and shapes are formed. At the initial

stage, the film behaves as a dielectric, and upon a gradual increase in the amount of deposited metal, such distinct particles start to form clusters or fractals. At a phase transition point, a continuous path forms across the substrate, and thereby the film becomes metallic. The condition at which this phase transition from dielectric to metal occurs is known as percolation.<sup>25</sup> With random nanoparticles resonating at different wavelengths, the SMF can absorb and/or reflect in the broad spectral range from the UV to far-infrared.<sup>26</sup> Upon light illumination, the metal nanoparticles resonate at specific optical frequencies due to the coupling of the electromagnetic field and excitation of collective oscillations of electrons known as localized surface plasmon resonance. Hence, electromagnetic energy can be concentrated around these metal nanoparticles in ‘hot spots’, in which the electric field can be orders of magnitude higher than in other parts of the film.<sup>27–32</sup> Thus a laser beam focused on the surface of SMFs, or plasmonic aggregates can cause localized heating of metallic nanostructures near the hot spots,<sup>32–35</sup> and result in spatially selective melting, reshaping or fragmentation of the metal film.<sup>36–40</sup> As a result, spectrally and polarization selective changes occur in the transmittance, reflectance and absorption spectra due to these structural changes.<sup>24,37,40–43</sup> A gradual change in the optical spectra then allows for a change in colors in response to the modification of the nanoparticles and their corresponding absorption and scattering at different wavelengths. Such an inexpensive, simple, and environment-friendly method of color generation has been recently demonstrated with single-layer SMFs and with the SMFs deposited over a dielectric spacer on top of a metallic backplane mirror<sup>44</sup> to show promising results for macroscopic printing applications.<sup>22–24,35,44</sup> Laser printing on other plasmonic random<sup>6,45–50</sup> and ordered<sup>51</sup> structures have also been recently reported.

In this paper, we report studies of plasmonic colors of a structure made of an optically thick silver film (a mirror) deposited on a glass substrate, followed by a thin dielectric (silica, SiO<sub>2</sub>) spacer and a silver SMF. We refer to such structures as the semicontinuous metal films on the

mirror (SMF/M). We employ the dielectric spacer and mirror to utilize the gap-plasmon mode–coupling of the SMF’s nanoparticles with the metallic mirror.<sup>52</sup> Although we have already initially explored this structure,<sup>24,53–55</sup> neither a thickness dependence nor optimization of colors has been studied. In this paper, we aim at the overall optimal design that generates the widest gamut of non-fading vibrant colors and addresses the crucial problem of the chemical stability of the Ag SMFs using a dielectric coating. We explore the coating fabricated with either the conventional method of electron-beam evaporation or atomic layer deposition (ALD). The final fabrication technique developed within this effort is lithography-free; it overcomes the core disadvantages of expensive electron-beam lithography for the generation of colors. Due to a very thin overcoating layer, the thickness of the entire structure is on the order of one hundred nanometers ( $\sim 150$  nm). It can be deposited on any substrate that can sustain the thermal heating due to laser illumination ( $5 \text{ mJ/cm}^2$  to  $400 \text{ mJ/cm}^2$ ). The fabrication approach requires less quantity of chemical elements for the overall process compared to other macroscopic printing techniques. Furthermore, it overcomes the drawback of a lower resolution in lithography-free color generation techniques with a beam size of  $0.3 \text{ mm}$  that can be decreased even further based upon the purpose of a given application. Finally, we present several fine-art pieces, using our in-house laser photomodification setup, laser-printed on the SMF/Ms and protected with the ultra-thin dielectric coating. The paper has been organized as follows. First, we overview our SMF/M structure and in what ways we can optimize the structure in [Section 1](#). The optimized structures post-processed with laser photomodification for a wider gamut of colors are discussed in [Section 2](#). The durability of the proposed structures with stable colors is afterward addressed in [Section 3](#). Finally, fade-free artistic images are presented in [Section 4](#) as select application examples of such structures.

## RESULTS AND DISCUSSION

### 1. Dependence of the SMF/M color on the thickness of the top Ag SMF layer

Semicontinuous metal films are made of disordered nanoparticles of random size, shape, and position distributed over a substrate. The morphology of SMFs and metal filling factor strongly depend on the amount of metal mass deposited and details of the deposition process. Thus, the amount of the deposited mass can drastically alter the optical properties of the film, leading to a diverse color palette. Unfortunately, for a given metal, the possible colors from a single-layer SMF are somewhat limited<sup>24</sup>. Another approach to changing the optical spectra is through utilizing gap plasmon resonance between two metal layers separated by a relatively thin dielectric layer<sup>23,24,52</sup>. Such a structure has been studied in our previous study, where we have gap plasmon resonance between SMF nanostructures and a metallic mirror layer separated by a silica layer. The schematic view of the structure is shown in Figure 1. The structure comprised of an Ag SMF layer of thickness,  $t_{Ag} = 10$  nm with an overcoating layer of silica of thickness,  $t_c = 30$  nm. Although that structure showed stable colors, a sufficiently wide gamut was not achieved. Hence, optimization to accomplish a broad range of stable colors has been required.

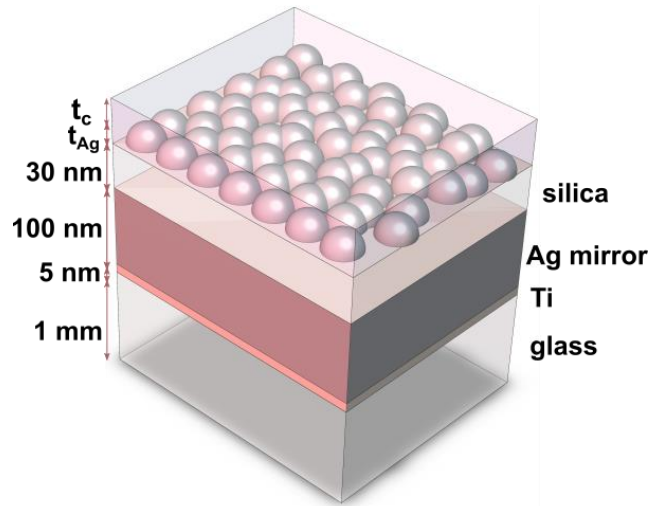


Figure 1. Schematic view of the SMF/M structure. The thickness of the top Ag SMF layer is  $t_{Ag}$  and the thickness of the overcoating layer is  $t_c$ , the thickness of the substrate is scaled to fit the figure.

Hence, to widen the spectra of obtained colors for the proposed structure, the first step is to change the Ag SMF layer to explore the correspondence between the deposited metal nanoparticles and the resulted optical spectra. From<sup>24</sup>, we know that for the SMF/M type structures,  $t_{Ag} \geq 17$  nm results in Ag films above percolation with a metallic optical response, showing substantial reflectance. Moreover, upon the photomodification, the laser-induced heat in the hot spots in such film, instead of being absorbed locally, is dissipated over the film, due to the numerous continuous metallic paths facilitating the heat transfer. Moreover, the SMF/Ms of that class also show low spectral and spatial selectivity when modified. Hence, we decided to analyze the structures below percolation, with  $t_{Ag} < 17$  nm, for which the incident energy is absorbed locally, mainly close to the hot spots around the Ag nanoparticles. In such a case, there will be limited heat transfer from the areas of the hotspot as the film below percolation is made of isolated nanostructures.

Figure 2a shows the reflectance spectra for the Ag SMF thickness for a range of  $t_{Ag} = 5 - 17$  nm. Corresponding visible colors are also shown in parallel along with the SEM images that show the relationship between the metal filling factor and the optical spectra. We see that, with the increasing thickness, the size of the metal nanoparticles changes, corresponding to the change in the absorption and reflected color. Initially, we have been unable to achieve robust SMFs with  $t_{Ag} \leq 5$  nm, due to their intrinsic chemical instability. Although vibrant colors could be achieved at lower Ag thickness (Figure 2a), due to the inherent oxidizing nature of Ag<sup>56</sup>, those SMF/M quickly (in a matter of days) have been losing their initial color. Hence, we protect the structures with a silica layer of thickness,  $t_c = 30$  nm. The silica protected structures demonstrated high stability compared to the uncoated ones. Moreover, the protective silica coating shifts the resonances of SMF nanostructures to longer wavelengths, producing the reflected colors in the blue region (Figure 2b). The corresponding CIE 1931 color diagram

of uncoated and coated SMF/Ms is shown in Supplementary Information (Figure S1). These initial colors of the coated SMF/M structures open new possibilities of obtaining different colors through post-laser modification for tunable spectral selectivity.

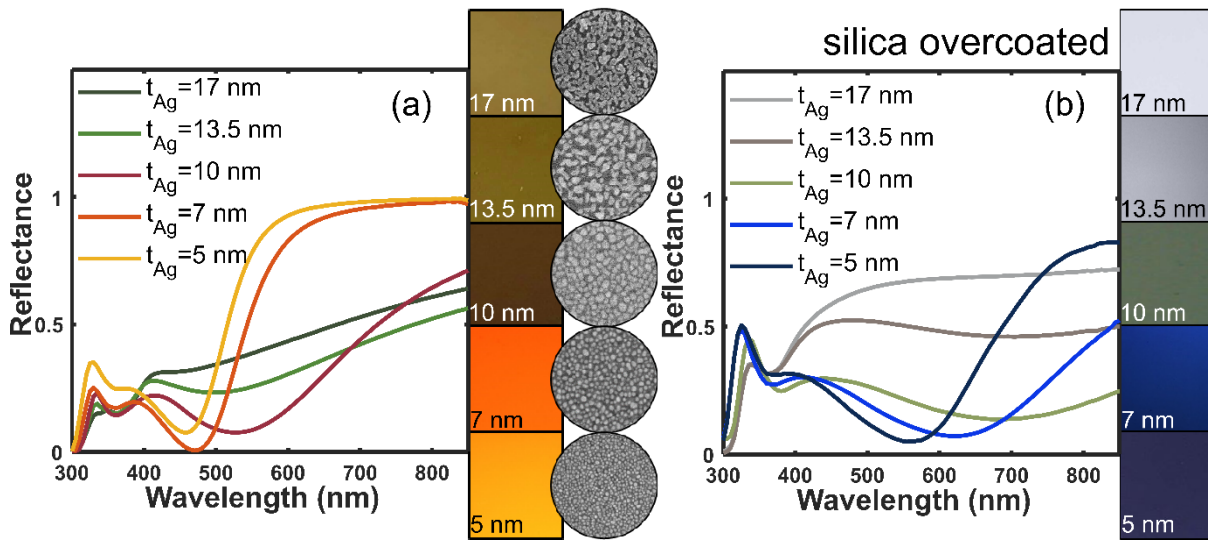


Figure 2. Reflectance spectra of Ag SMF/M structures with different Ag thicknesses ( $t_{Ag}$ ) along with their corresponding colors for (a) without and (b) with the 30 nm silica overcoating layer. As the SMF Ag film thickness increases we first see an increase in absorption, manifesting as a dip in reflectance, and next, there is a decrease in absorption where the layer (higher thickness) becomes gradually metallic. The color squares are the SMF/M surface images captured using an optical microscope with 10x objective lens (Nikon Eclipse, L150). Corresponding SEM images are also inserted in parallel which show the change in the film structure as the Ag thickness increases. Diameter of the SEM circled image is 0.4  $\mu\text{m}$ .

## 2. Laser color printing on SMF/M

The fabricated SMF/M structures were next subjected to laser post-processing for inducing spectrally selective changes in the optical spectra. Irradiating the SMF/M samples with the laser beam resulted in a significant rise in temperature of resonating nanostructures<sup>57</sup>. This effect resulted in melting and fragmenting the nanoparticles, eventually altering the optical properties of the SMF/M structure. From Fig. 2, we see that for  $t_{Ag} > 10$  nm, the SMF/M structures are quite reflective, and hence laser post-processing will not be able to induce changes in the absorption spectra. Therefore, laser modification is conducted on samples with  $t_{Ag} \leq 10$  nm.

For laser post-processing, we use linearly polarized femtosecond laser pulses (repetition rate 1 kHz, pulse duration 80 fs, wavelength 800 nm) to modify some of the fabricated SMF/Ms. In all laser modified cases, the laser beam is focused by a single lens to 0.3 mm diameter ( $1/e^2$ ). The scanning speed is maintained at 3 mm/s. A few mm<sup>2</sup> area is uniformly photomodified in the ambient atmosphere employing scanning of the sample with the laser beam by placing the sample on a XYZ computer-controlled stage. To ensure uniformity of modification over the large area we use 50  $\mu$ m Y-axis (raster) step.

The results of laser modification on the SMF/M sample with Ag thickness,  $t_{Ag} = 7$  nm are presented in Figure 3. Results for  $t_{Ag} = 10$  and 5 nm are presented in Supplementary Information (Figure S2 and Figure S3). The laser fluence is gradually increased with the above-mentioned laser parameters from 5 mJ/cm<sup>2</sup> to the value of damage threshold (on the order of 200 mJ/cm<sup>2</sup>). The corresponding reflectance spectra was then measured using a spectrometer equipped with an integrating sphere (see Fig. 3a, Fig. S2a, and Fig. S3a). From the changes of the reflectance spectra of SMF/M samples illuminated with the laser, we draw several conclusions. A “step function” type response in the visible (in reflectance) is observed after photomodification. As the laser fluence increases, the “transition point” of the step function moves to shorter wavelengths. We attribute such behavior of the reflectance to the following effects. As the fluence of the illuminating laser beam increases, the nanostructured elements of the top Ag SMF gradually fragment and morph into spherical nanoparticles<sup>39</sup>; the absorption at the longer wavelengths decreases, and reflectance reaches a value close to unity (Fig. 3 and Supplementary Information, Fig. S4). Thus, the SMF/M for the long wavelengths behaves as a metallic mirror protected with a dielectric layer. At the same time (at low fluences), there is an increase of absorption at short wavelengths due to the formation of new nanostructures absorbing at short wavelengths. Photoinduced damage of the bottom silver mirror occurs at the fluences above 200 mJ/cm<sup>2</sup>. These induced changes in the optical spectra then result in a wide



range of reflected colors. We have seen similar behavior of SMF/M structures upon laser illumination in our earlier paper also<sup>24</sup>, but the generated color gamut was comparatively low. We can observe a broader color gamut from the CIE 1931 color map, which has been generated from the corresponding reflectance spectra from  $t_{\text{Ag}} = 7$  nm in Fig. 3b. Here, we are able to obtain colors from blue to yellow, whereas earlier<sup>24</sup> the gamut was limited to orange, and the colors for shorter wavelengths were also not achieved (Supplementary Information, Fig. S5). From the CIE color maps for each case (Fig. 3b and Supplementary Information, Fig. S2b and Fig. S3b), we observed that, the Ag SMF/M with thickness,  $t_{\text{Ag}} = 7$  nm gives the widest range from blue to green, red, and yellow.

Although the initial tests for the silica protective coating ( $t_c = 30$  nm) conducted on the Ag SMF/M sample with  $t_{\text{Ag}} = 10$  nm ensured chemical stability<sup>24</sup>, such a protective layer appears to be inadequate for lower Ag SMF thicknesses ( $t_{\text{Ag}} = 5$  and 7 nm) to abate oxidation/sulfidation completely, as those structures degrade over time. Hence, it is necessary to additionally optimize the protective layer to achieve chemical stability and color vibrancy in SMF/Ms with  $t_{\text{Ag}} < 10$  nm.

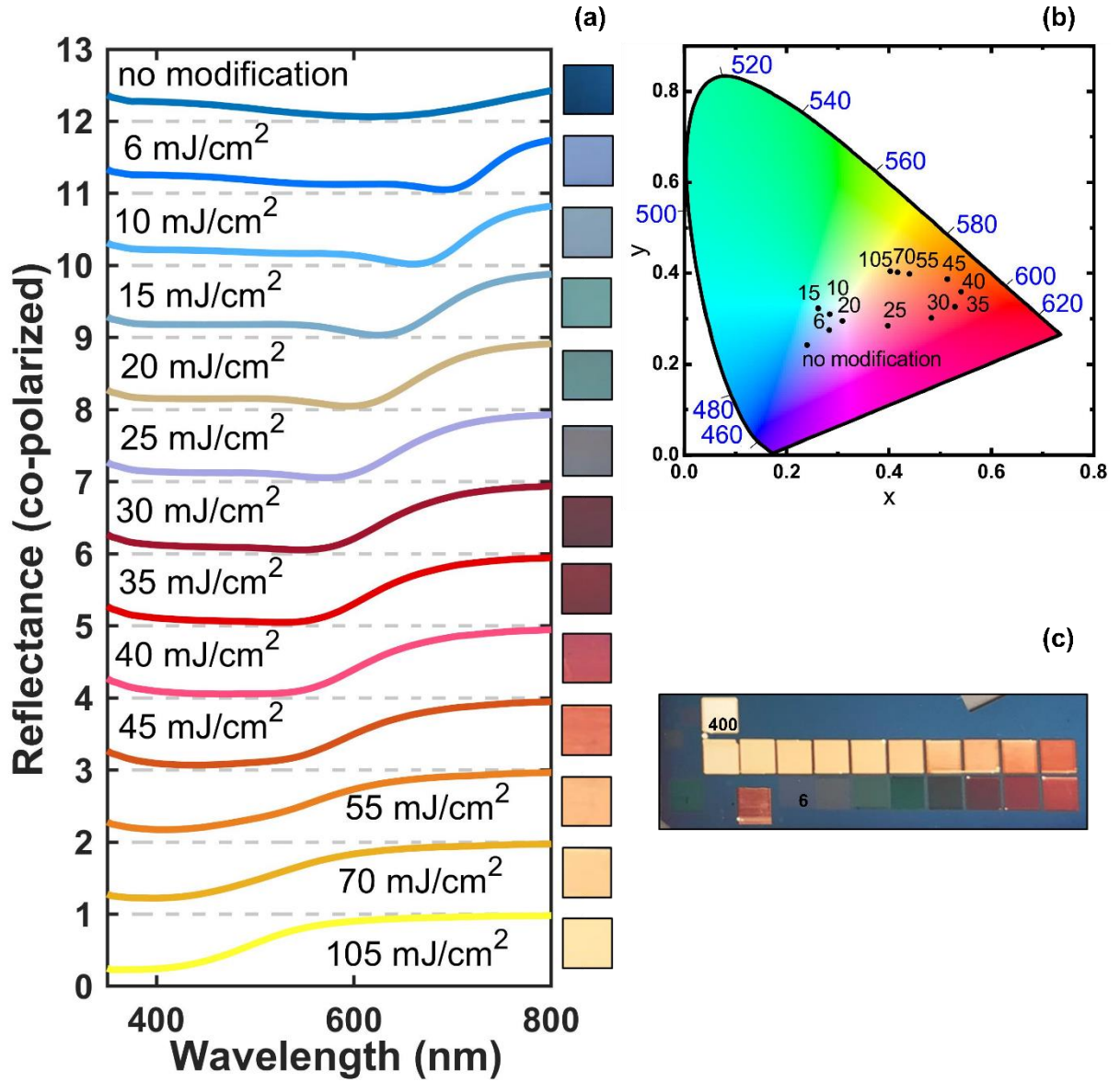


Figure 3. Laser modification of Ag SMF/M ( $t_{Ag} = 7$  nm) with a silica protective coating,  $t_c = 30$  nm. (a) Reflectance spectra and (b) corresponding CIE 1931 color diagram of areas photomodified with different laser fluence measured with linearly polarized light co-polarized (cross-polarized in Supplementary Information, Fig. S6) with respect to the laser polarization. The inset squares represent the generated color palette recorded using unpolarized light. (c) Optical image of different photomodified squares from 6 mJ/cm<sup>2</sup> (marked '6') to 400 mJ/cm<sup>2</sup> (marked '400').

### 3. SMF/M stability studies

We took two possible approaches to address the issue of chemical stability over time. One possibility was to further increase the thickness of the protective silica coating to sustain chemical damage. Henceforth, in order to comprehend the range and limitations of this

approach, we initially performed numerical simulations with a commercially available 3D finite-difference time-domain (FDTD) solver (Lumerical Inc., FDTD Solutions)<sup>58</sup>. To precisely retrieve the optical response of the random Ag SMF films, the binarized SEM images of the fabricated film have been imported into the simulation domain using a build-in Lumerical material import parser. We extracted the relative permittivities of Ag and silica through spectroscopic scan using a J. A. Woollam V-Vase UV-vis-NIR spectroscopic ellipsometer. The optical response of the SMF type films depends on the distribution of the plasmonic particles of different sizes. Hence, the response of the structure should be statistically averaged over a sufficiently large number of realizations. Thus, we select 25 distinct regions with an area of  $500 \times 500 \text{ nm}^2$  at various spots of the same sample. The overall response of the SMF film is assessed by averaging the power transmission/reflection coefficients over these realizations. This simulation approach is similar to our previous studies on semicontinuous metal films<sup>24,40,59</sup>, except for the use of the commercial software and better automation of the image processing and geometry parsing process.

The simulations are performed for the Ag SMF/M structure with  $t_{\text{Ag}} = 10 \text{ nm}$  with a gradual increase in the thickness of the overcoating silica layer from  $t_c = 30 \text{ nm}$  to  $t_c = 90 \text{ nm}$  and then experimentally tested (Supplementary Information, Fig. S7a and Fig. S7b). The experimental data corroborated our simulations. Also, the thick silica overcoating layer ( $t_c = 90 \text{ nm}$ ) showed a redshift in the resonance dip and a broadening of spectrum similar to the simulation results (Supplementary Information, Fig. S7). Unfortunately, with a thick overcoating layer, laser modification produces lower saturation and hue of colors (Supplementary Information, Fig. S7c and Fig. S7d). Although we tested the chemical stability of the thick silica overcoating layer ( $t_c = 90 \text{ nm}$ ) by measuring the reflectance spectrum of the freshly fabricated sample and remeasured after eleven months (Supplementary Information, Fig. S8), such a low vibrancy has been a critical impediment towards using a more robust thick

silica overcoating layer. Moreover, an overall structure that is relatively thin is also desired for scalable production with less materials.

Another possibility of looking at this problem is to change the bottom-up coating technique for passivation, which might not seal the three-dimensional Ag nanoparticles of top SMF properly, leaving areas shadowed and less immune to chemical reactions. Atomic layer deposition is an effective method of passivation of nanostructures that yields conformal thin films<sup>60,61</sup> at low temperatures. Our Ag sample is also susceptible to temperature variance, and ALD provides an additional benefit of thin layer deposition at low temperatures<sup>62</sup>.

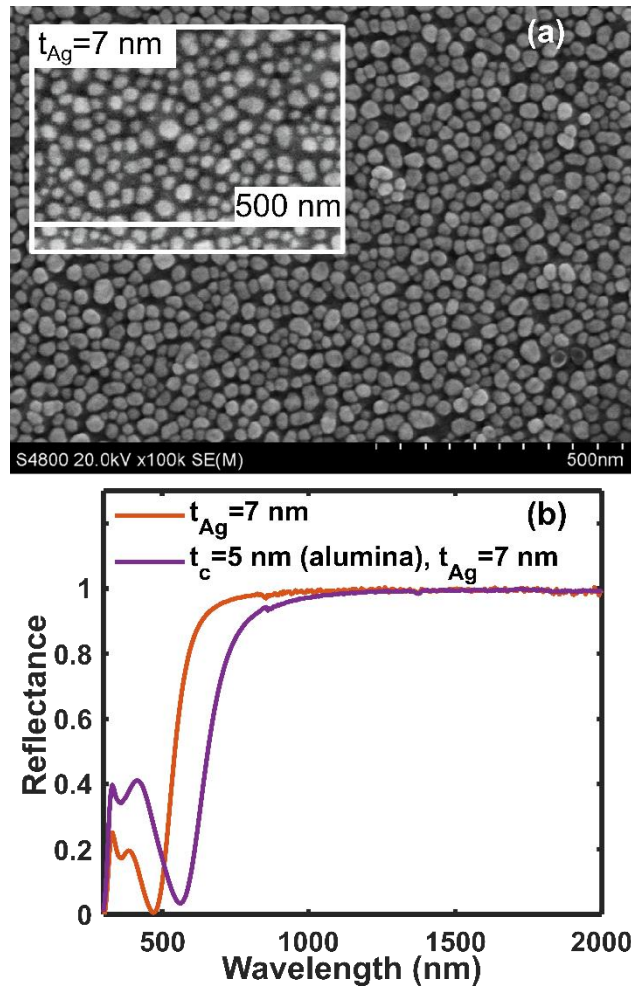


Figure 4. (a) SEM image of the Ag SMF/M ( $t_{\text{Ag}} = 7$  nm) with an alumina protective coating,  $t_{\text{c}} = 5$  nm. The inset shows an SEM image of uncoated Ag SMF/M with ( $t_{\text{Ag}} = 7$  nm) (b) Reflectance spectra of Ag SMF/M ( $t_{\text{Ag}} = 7$  nm) with and without an alumina protective coating.

Hence, we tested passivation of the SMF/M surface with a thin coating of alumina ( $\text{Al}_2\text{O}_3$ ) using ALD from TMA and water precursors. We fabricated Ag SMF/M ( $t_{\text{Ag}} = 7 \text{ nm}$ ) using the e-beam deposition process and then overcoated the structure with 5 nm of alumina. Figure 4a shows the SEM top view image of the alumina-coated Ag SMF/M ( $t_{\text{Ag}} = 7 \text{ nm}$ ). The alumina coating redshifts the optical spectra (Figure 4b) as expected due to a higher refractive index of alumina as compared to air. Before performing laser modifications on the alumina-coated structures, it is important to prove that such a thin protective layer can protect the Ag nanoparticles from degradation.

Henceforth, we corroborated the stability of the alumina coated SMF/M structure by comparing the reflectance spectra of Ag SMF/M ( $t_{\text{Ag}} = 7 \text{ nm}$ ) coated with  $t_c = 30 \text{ nm}$  (silica), which also gave vibrant colors, to Ag SMF/M ( $t_{\text{Ag}} = 7 \text{ nm}$ ) with the alumina coating,  $t_c = 5 \text{ nm}$  (Figure 5). The reflectance of those structures was measured (i) immediately after fabrication and (ii) after several months of storage in the ambient atmosphere. While we observe significant changes in the spectra (mainly shift of reflectance minimum to shorter wavelengths) for the SMF/M coated silica, negligible changes are kept for the alumina-coated SMF/M.

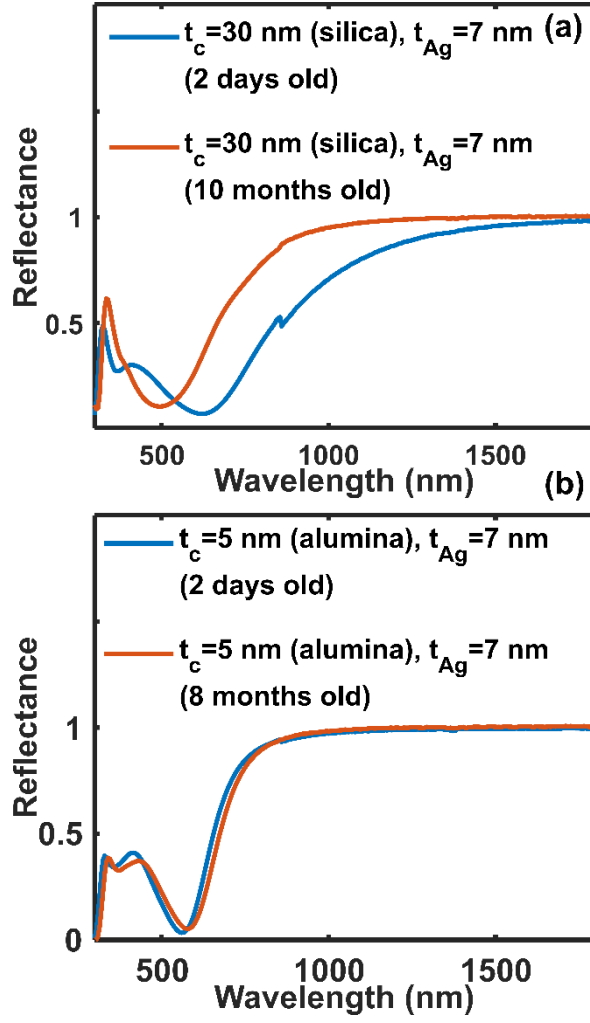


Figure. 5. Reflectance spectra of (a) Ag SMF/M with  $t_{Ag} = 7$  nm overcoated with  $t_c = 30$  nm (silica) and (b) Ag SMF/M with  $t_{Ag} = 7$  nm overcoated with  $t_c = 5$  nm (alumina). Both the samples were measured immediately after fabrication and after several months, as stated in the legend.

As the alumina-coated SMF/Ms demonstrated higher stability, we further explored the possibility of their laser modification for the generation of the broad color range. We followed the same procedure as for the silica-coated samples. Figure 6a shows the reflectance spectra of the Ag SMF/M with  $t_{Ag} = 7$  nm overcoated with  $t_c = 5$  nm (alumina) photomodified with various laser fluences from 10 to 250 mJ/cm<sup>2</sup>. Figure 6b presents the corresponding CIE map and Fig. 6c shows the camera image of the sample with beautiful bright colors. We see a similar trend of change in the reflectance spectra as the laser fluence is increased. At higher fluence (above 150 mJ/cm<sup>2</sup>), a saturated hue in the yellow region is observed (Fig. 6b) and a further

increase does not generate significant change in the color, but gradual damage of the bottom mirror occurs (above  $250 \text{ mJ/cm}^2$ ). Again, compared to our previous color gamut ranging from teal to orange (Supplementary Information, Fig. S4), we see a broader range from violet to yellow. The corresponding SEM images for different energy densities of the photomodified areas are presented in Figure 7. For the Ag SMF/M with  $t_{\text{Ag}} = 7 \text{ nm}$  overcoated with  $t_c = 5 \text{ nm}$  (alumina) also, there is a gradual transformation to spherical nanoparticles with increasing energy density. As we see in Fig. 7, the Ag nanoparticles have deformed and seemed to have been detached from the bottom layer, the alumina coated protective layer keeps the particles intact, showing the original extrusions of the particle shape<sup>61</sup>. We also checked the stability of the reflectance of a photomodified area and compared the results (Supplementary Information, Fig. S9). In all cases, the alumina coated structures have demonstrated superior stability as compared to  $t_c = 30 \text{ nm}$  (silica).

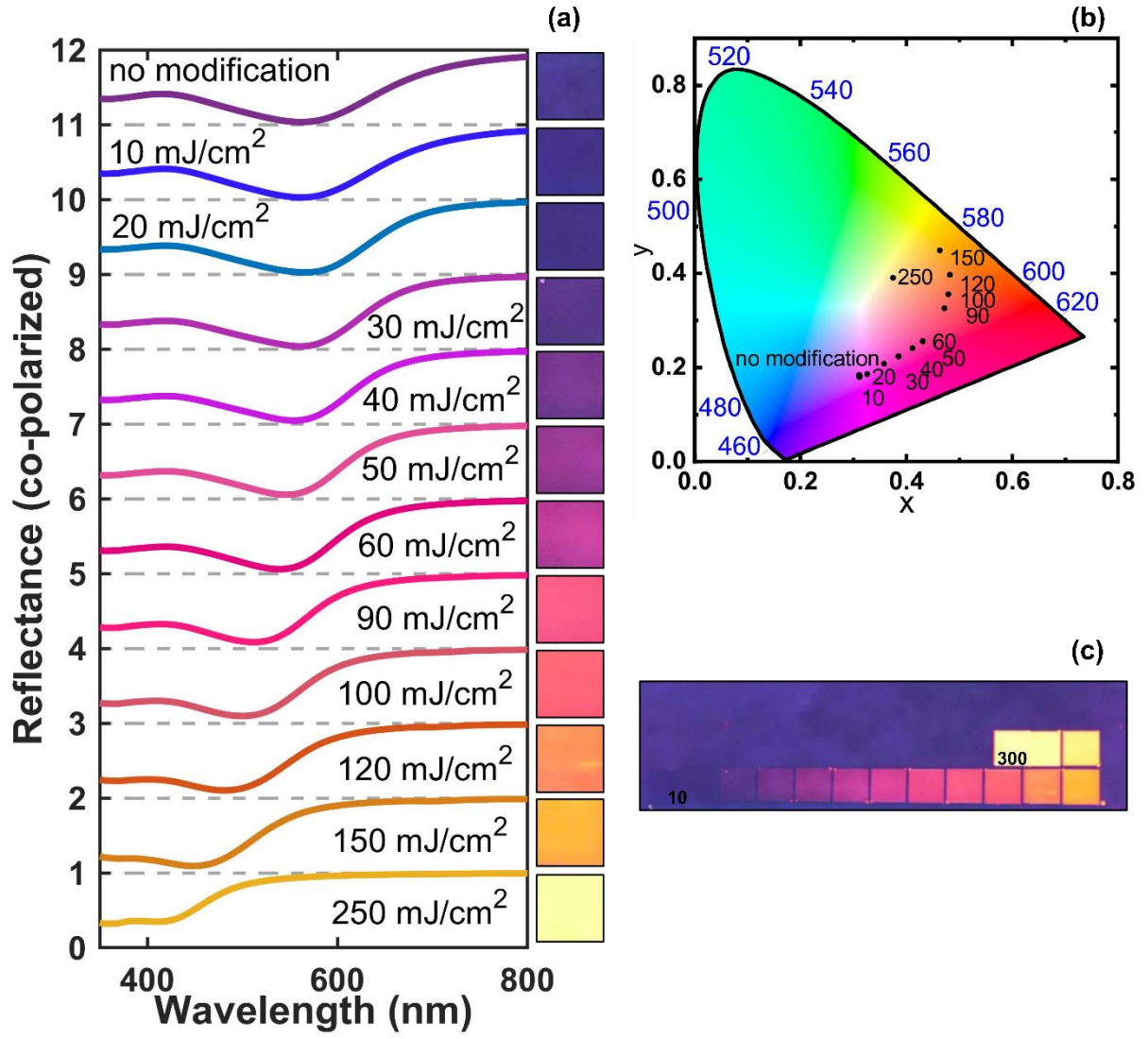


Figure 6. Laser modification of Ag SMF/M with  $t_{Ag} = 7$  nm overcoated with  $t_c = 5$  nm (alumina). (a) Reflectance spectra and (b) corresponding CIE 1931 color diagram of areas photomodified with different laser fluence measured with linearly polarized light co-polarized with respect to the laser polarization. The inset squares represent the generated color palette recorded using unpolarized light. (c) Optical image of different photomodified squares starting from 10 mJ/cm<sup>2</sup> (marked '10') to 300 mJ/cm<sup>2</sup> (marked '300').



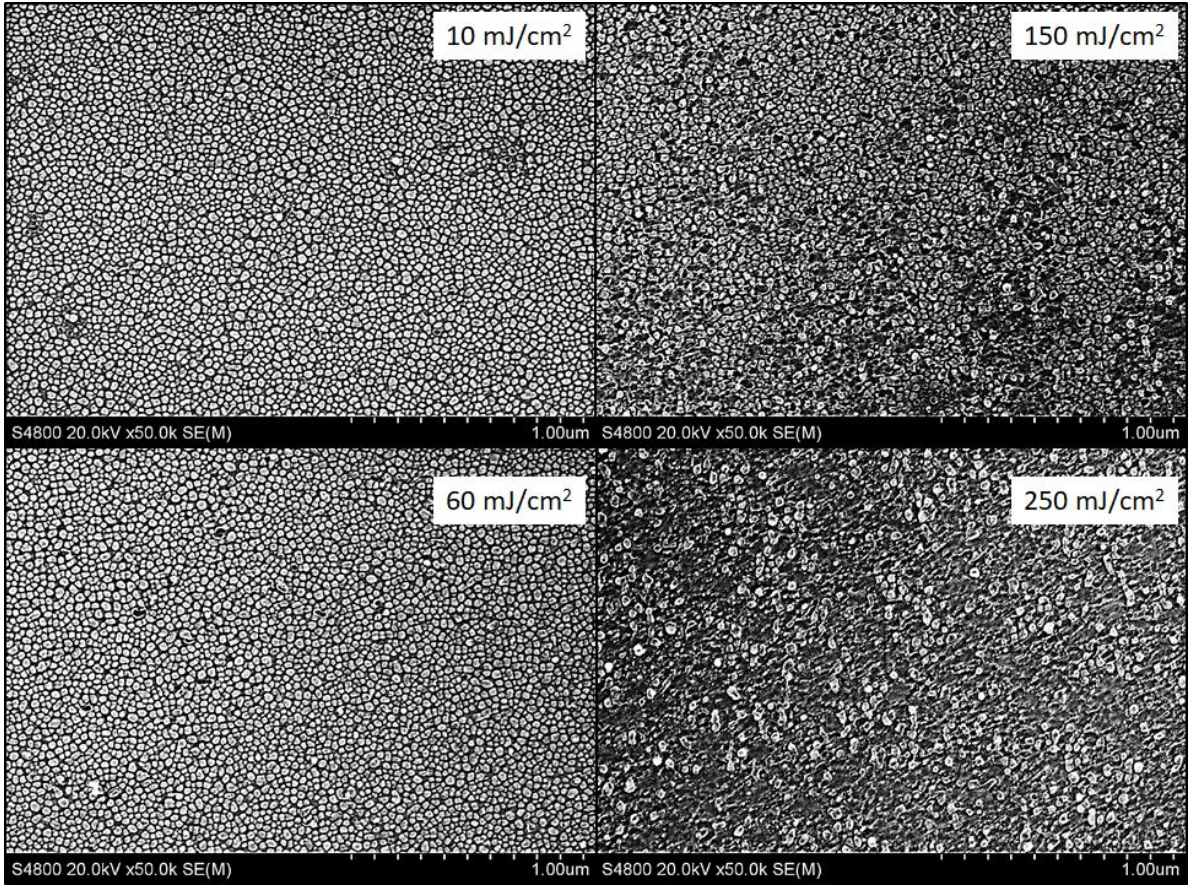


Figure 7. SEM images of Ag SMF/M with  $t_{Ag} = 7\text{nm}$  overcoated with  $t_c = 5\text{nm}$  (alumina) photomodified with different energy densities.

#### 4. Fine-art application

We tested different designs to explore the visual capabilities in terms of quality, resolution, and aesthetics of the Laser modification method. We reproduced different fine designs (Figure 8) with the in-home built laser scanning setup having a computer controlled motorized XYZ stage. The designs were converted in a bitmap format, which was fed into the interface with a Matlab script. The structure mounted to the stage was then raster-scanned with different laser fluences. The results of these visual experiments were exhibited at the Purdue 2050: Conference of the Future. The purpose of the conference was to discuss the technology of tomorrow and find sustainable solutions. We built an optical arrangement in the exhibit (Figs. 8a and 8b) that can project reflections at a bigger scale (24"×24") for a demonstration of merging future art and

science. The setup showcased different Mandala designs (Figs. 8c-g), which can be considered symbolic representations of the self and reflections of the universe<sup>63</sup>. We also reproduced other artifacts (Figs. 8h-j) using our laser setup for other artistic applications. This unique structure, along with the laser setup, can hence be applied to print any design on any substrate (rigid/flexible) that opens the potential for extensive research and real-life applications not just restricted to art.

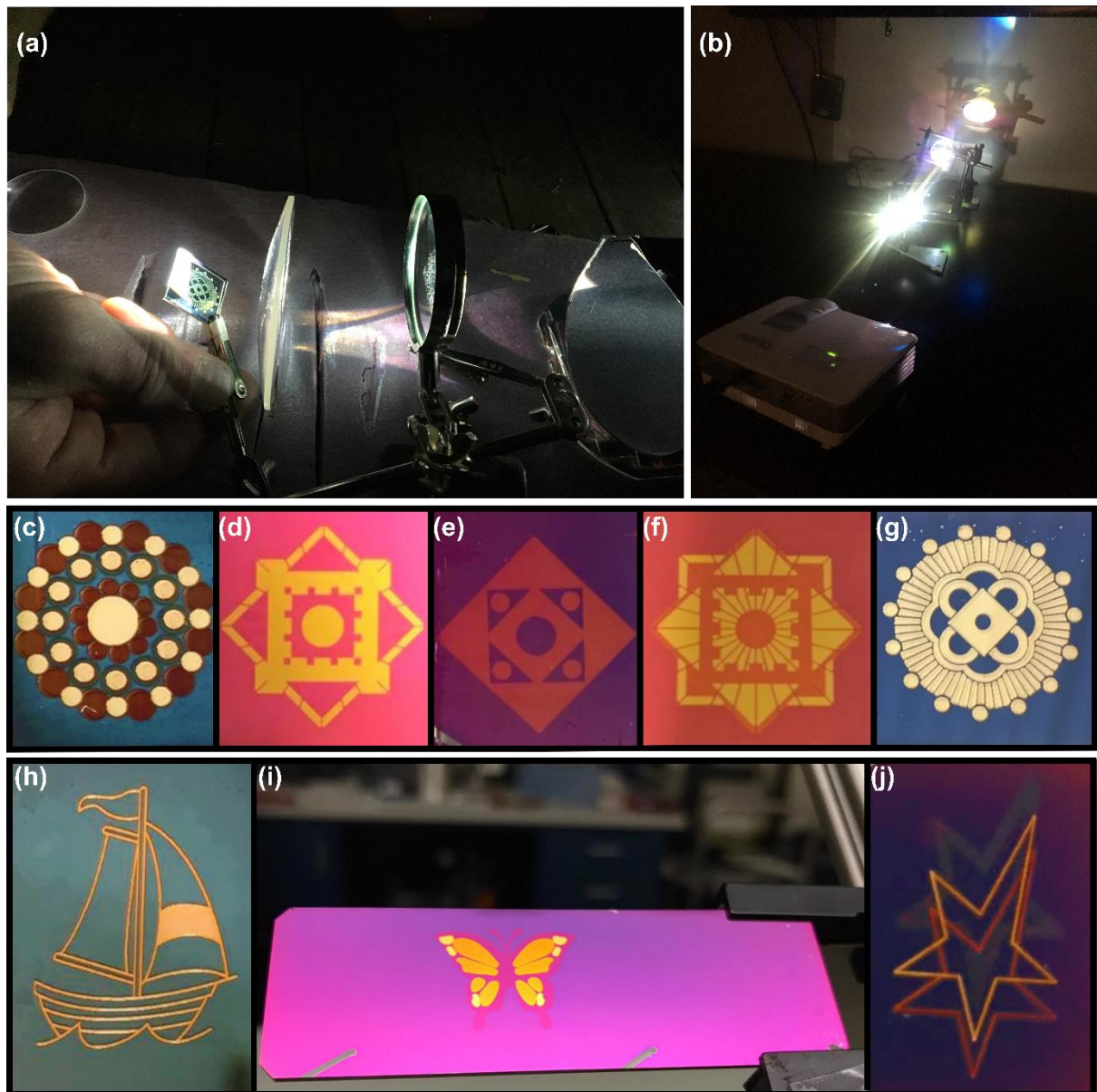


Figure 8. (a-b) Optical setup for projecting reflections from the surface of our fabricated sample at a bigger scale (24"×24"). (c-g) Different color images printed on Ag SMF/M. The designs (c-g) were produced as part of the exhibit titled ‘Plasmonic



Mandalas' in Purdue 2050: Conference on the Future ([The Exhibit](#)). A demonstration of the magnified dimension has been recorded here ([Plasmonic Mandalas](#)).

## CONCLUSION

Random metal nanoparticles of inhomogeneous sizes and shapes comprising the semicontinuous metals films (SMF) can demonstrate a wide variety of colors depending on the deposition mass. In this paper, we demonstrated that semicontinuous metal films with a dielectric spacer on a mirror (SMF/M) could be designed for macroscopic color applications through varying the Ag thickness ( $t_{\text{Ag}} = 5 - 17 \text{ nm}$ ). The chemical stability of Ag films is achieved with protective coatings, either with a relatively thick silica layer ( $t_c = 30 \text{ nm}$  and  $90 \text{ nm}$ ) or a thin layer of ALD coated alumina ( $t_c = 5 \text{ nm}$ ), and are validated with measurements after a long time exposure to air. Laser illumination (1 kHz, 80 fs, 800 nm, linear polarization) on SMF/M with different energy densities ( $6 - 250 \text{ mJ/cm}^2$ ) has then been demonstrated to show a broad range of colors from blue to red to yellow by causing changes in the optical spectra through thermally-induced changes in the shape and size of the random Ag nanoparticles. We also proved the long term stability of laser-modified SMF/Ms, which enabled us to design their broad, robust, and non-fading color gamut. SMF/M structures have the potential for a much broader range of colors presented here, depending on the combination of different materials and their respective thicknesses. A more rigorous study can be conducted on the effect of different materials like surrounding media (dielectrics) on the localized thermal heating of plasmonic nanoparticles, for example, through thermal reflectance measurements. Laser post-processing can be further optimized by varying other laser parameters such as line spacing, scanning speed, exposure time, beam size, etc. that can increase the overall color palette. Moreover, more advanced artistic designs and technological applications that require higher resolution are achievable through this optical setup for real-life plasmonic color applications.

## METHODS

**Fabrication of SMF/M structures.** The SMF/M structures formed from a silver SMF, silica spacer, and a silver mirror deposited on a glass substrate were fabricated in a single process using an electron-beam physical vapor deposition (PVD) technique. The glass substrates were pre-cleaned with Piranha solution (3 parts  $\text{H}_2\text{SO}_4$ :1 part  $\text{H}_2\text{O}_2$ ) for 15 minutes and thoroughly rinsed with distilled water. After drying out with nitrogen gas, the substrates were then sonicated in solvents (toluene, acetone, and isopropyl alcohol) and dried thoroughly. Next, an Ag SMF, silica spacer, silver mirror, and titanium adhesion layer were deposited in a high-vacuum deposition chamber (PVD Products, Inc., base pressure  $2.6 \times 10^{-6}$  torr) at room temperature. Silicon dioxide ( $\text{SiO}_2$ , 99.99% purity), titanium (Ti, 99.99% purity), and silver (Ag, 99.99% purity) from the Kurt J. Lesker Company were used for fabricating all structures. The deposition rate (1 Å/s for all materials) and layer thickness were monitored with a quartz crystal microbalance. The protecting layer on top of the structure was deposited in two ways: electron beam evaporation and atomic layer deposition. The silica overcoating layer was deposited within the same process in the PVD chamber. The atomic layer deposition (ALD) was used to deposit a thin protective layer of alumina at 100 °C. In the ALD process, trimethylaluminum (TMA,  $\text{Al}(\text{CH}_3)_3$ ) and water ( $\text{H}_2\text{O}$ ) were alternately entrained with an argon carrier flow using gas switching valves.

The process of forming a monolayer of alumina started with pumping TMA pulse for 0.06 s. At this step, TMA reacted with the hydroxylated surface of SMF/M after exposure to air to form -OH bonds resulting in a monolayer. The unreacted molecules of TMA were then purged with argon carrier gas for 10 s. Water with a pulse of 0.06 s is afterward pulsed. That process removed the  $\text{CH}_3$  groups, creates Al-O-Al bridges, so that a passivated-surface with Al-OH.  $\text{CH}_4$  (methane) was formed as a gaseous byproduct at the end of this step. The

unreacted H<sub>2</sub>O and CH<sub>4</sub> molecules were purged for 10s. This step ended a single cycle. One cycle resulted in the deposition of approximately 1 Å of alumina.

**Laser post-processing and design setup.** Laser processing on the SMF/Ms was performed in an ambient atmosphere using an ultrafast Ti:Sapphire femtosecond laser (Spectra-Physics, Solstice Ace; 1 kHz, 80 fs, 800 nm, linear polarization). The laser beam was focused using a single lens and the  $1/e^2$  gaussian beam size was determined using the knife-edge technique. To print areas of uniform color, samples were mounted on a motorized XYZ stage (Zaber Technologies Inc.) capable of raster scanning and controlled with a computer interface. The scanning speed was maintained at 3 mm/s. A Matlab generated code for the Zaber XYZ stage control toolbox was used to print different designs on the samples. We used an optical microscope (Nikon Eclipse, L150) as well as a general camera to capture the color images of printed structures.

**Sample characterization.** A field emission scanning electron microscope (FESEM, Hitachi S-4800) was used to characterize the nanostructure of uncoated SMFs. The semicontinuous metal films of SMF/M overcoated with 30 nm and 90 nm silica layer were not characterized with SEM; it was not possible to visualize the metallic nanostructures through a relatively thick silica layer. In contrast, the SEM images for the case of the SMF/Ms with Al<sub>2</sub>O<sub>3</sub> coatings were recorded, as these protective layers were significantly thinner. Total transmittance and total reflectance spectra of as-fabricated and photomodified structures were measured using a spectrophotometer (Perkin Elmer, Lambda 950) equipped with an integrating sphere (150 mm) module (8 deg. angle of incidence used for reflectance measurement) and polarizers. Spectralon was used as a reference sample for reflectance measurements. The calculation of CIE 1931 color coordinates from reflectance spectra was performed with ORIGIN™ software<sup>64,65</sup>.

Supporting Information 1 Available: This material is available free of charge via the Internet at <http://pubs.acs.org>.

- CIE 1931 color diagram of variable Ag thickness of semicontinuous metal film with mirror (Ag) and dielectric spacer ( $\text{SiO}_2$ ) (SMF/M) with and without the overcoating  $\text{SiO}_2$  layer.
- Laser modification of Ag SMF/M with  $t_{\text{Ag}} = 10$  nm overcoated with  $t_c = 30$  nm (silica)
- Laser modification of Ag SMF/M with  $t_{\text{Ag}} = 5$  nm overcoated with  $t_c = 30$  nm (silica)
- Reflectance spectra (longer wavelength) of Ag SMF/M with  $t_{\text{Ag}} = 7$  nm overcoated with  $t_c = 30$  nm (silica)
- CIE 1931 color diagram of 30 nm overcoated 10 nm Ag SMF/M from reference<sup>24</sup>.
- CIE 1931 color diagram of Ag SMF/M with  $t_{\text{Ag}} = 7$  nm overcoated with  $t_c = 30$  nm (silica) (cross-polarized reflectance measurement)
- Reflectance spectra (simulated and experimental) of variable top silica layer of Ag SMF/M with  $t_{\text{Ag}} = 7$  nm for stable structures. Laser modification of Ag SMF/M with  $t_{\text{Ag}} = 10$  nm overcoated with  $t_c = 90$  nm (silica)
- Stability test on Ag SMF/M with  $t_{\text{Ag}} = 10$  nm overcoated with  $t_c = 90$  nm (silica)
- Stability test on one of the photomodified areas of Ag SMF/M with  $t_{\text{Ag}} = 7$  nm overcoated with  $t_c = 30$  nm (silica) and  $t_c = 5$  nm (alumina)

Supporting Information 2 Available: This material is available free of charge via the Internet at <http://pubs.acs.org>.

- YouTube video link for the demonstration at the exhibit of Purdue 2050: Conference on the Future (<https://youtu.be/J1yrmwz493Y>)

## AUTHOR INFORMATION

### Corresponding Author

[piotr.nyga@wat.edu.pl](mailto:piotr.nyga@wat.edu.pl)

2 Kaliskiego St, Warsaw, 00-908, Poland

[aeb@purdue.edu](mailto:aeb@purdue.edu)

1205 W State St, West Lafayette IN, 47907, USA

### Author Contributions

P.N. conceived the idea of the laser color printing on SMF/M structures. S.N.C. and P.N. performed fabrication and optical characterization, data analysis and wrote the initial draft. S.N.C. did the SEM characterization. E.G. and S.N.C. prepared designs of images for laser printing, Z.K. performed FDTD simulations. P.N. S.N.C. and A.S.L. performed laser modification. P.N., A.B., A.V.K., and V.M.S. supervised the project.

All authors analyzed and discussed the results and participated in the preparation of manuscript.

### Funding Sources

Purdue team acknowledge financial support by the Air Force Office of Scientific Research grant FA9550-17-1-0243. PN acknowledges financial support by the Military University of Technology UGB 502-6700-23-759 grant and Fulbright Senior Award Scholarship awarded by the Polish-U.S. Fulbright Commission.

## REFERENCES

- (1) Hunt, R. W. G.; Pointer, M. R. *Measuring Colour*, Fourth.; Wiley, 2011.

<https://doi.org/10.1002/9781119975595>.

- (2) Yahagi, T.; Degawa, M.; Seino, Y.; Matsushima, T.; Nagao, M.; Sugimura, T.; Hashimoto, Y. Mutagenicity of Carcinogenic Azo Dyes and Their Derivatives. *Cancer Lett.* **1975**, *1*, 91–96. [https://doi.org/10.1016/S0304-3835\(75\)95563-9](https://doi.org/10.1016/S0304-3835(75)95563-9).
- (3) Ali, H. Biodegradation of Synthetic Dyes—A Review. *Water, Air, Soil Pollut.* **2010**, *213* (1–4), 251–273. <https://doi.org/10.1007/s11270-010-0382-4>.
- (4) Freestone, I.; Meeks, N.; Sax, M.; Higgitt, C. The Lycurgus Cup — A Roman Nanotechnology. *Gold Bull.* **2007**, *40* (4), 270–277. <https://doi.org/10.1007/BF03215599>.
- (5) Barchiesi, D. Lycurgus Cup: Inverse Problem Using Photographs for Characterization of Matter. *J. Opt. Soc. Am. A* **2015**, *32* (8), 1544. <https://doi.org/10.1364/JOSAA.32.001544>.
- (6) Zijlstra, P.; Chon, J. W. M.; Gu, M. Five-Dimensional Optical Recording Mediated by Surface Plasmons in Gold Nanorods. *Nature* **2009**, *459* (7245), 410–413. <https://doi.org/10.1038/nature08053>.
- (7) Lochbihler, H. Colored Images Generated by Metallic Sub-Wavelength Gratings. *Opt. Express* **2009**, *17* (14), 12189. <https://doi.org/10.1364/OE.17.012189>.
- (8) Goh, X. M.; Ng, R. J. H.; Wang, S.; Tan, S. J.; Yang, J. K. W. Comparative Study of Plasmonic Colors from All-Metal Structures of Posts and Pits. *ACS Photonics* **2016**, *3* (6), 1000–1009. <https://doi.org/10.1021/acsphotonics.6b00099>.
- (9) Kristensen, A.; Yang, J. K. W.; Bozhevolnyi, S. I.; Link, S.; Nordlander, P.; Halas, N. J.; Mortensen, N. A. Plasmonic Colour Generation. *Nat. Rev. Mater.* **2017**, *2* (1), 16088.



<https://doi.org/10.1038/natrevmats.2016.88>.

- (10) Song, M.; Kudyshev, Z. A.; Yu, H.; Boltasseva, A.; Shalaev, V. M.; Kildishev, A. V. Achieving Full-Color Generation with Polarization-Tunable Perfect Light Absorption. *Opt. Mater. Express* **2019**, 9 (2), 779. <https://doi.org/10.1364/ome.9.000779>.
- (11) Song, M.; Wang, D.; Peana, S.; Choudhury, S.; Nyga, P.; Kudyshev, Z. A.; Yu, H.; Boltasseva, A.; Shalaev, V. M.; Kildishev, A. V. Colors with Plasmonic Nanostructures: A Full-Spectrum Review. *Applied Physics Reviews*. American Institute of Physics Inc. October 25, 2019, p 041308. <https://doi.org/10.1063/1.5110051>.
- (12) Daqiqeh Rezaei, S.; Dong, Z.; You En Chan, J.; Trisno, J.; Ng, R. J. H.; Ruan, Q.; Qiu, C.-W.; Mortensen, N. A.; Yang, J. K. W. Nanophotonic Structural Colors. *ACS Photonics* **2020**. <https://doi.org/10.1021/acsphotonics.0c00947>.
- (13) Xu, T.; Wu, Y.-K.; Luo, X.; Guo, L. J. Plasmonic Nanoresonators for High-Resolution Colour Filtering and Spectral Imaging. *Nat. Commun.* **2010**, 1 (5), 1–5. <https://doi.org/10.1038/ncomms1058>.
- (14) Kumar, K.; Duan, H.; Hegde, R. S.; Koh, S. C. W.; Wei, J. N.; Yang, J. K. W. Printing Colour at the Optical Diffraction Limit. *Nat. Nanotechnol.* **2012**, 7 (9), 557–561. <https://doi.org/10.1038/nnano.2012.128>.
- (15) Si, G.; Zhao, Y.; Lv, J.; Lu, M.; Wang, F.; Liu, H.; Xiang, N.; Huang, T. J.; Danner, A. J.; Teng, J.; et al. Reflective Plasmonic Color Filters Based on Lithographically Patterned Silver Nanorod Arrays. *Nanoscale* **2013**, 5 (14), 6243. <https://doi.org/10.1039/c3nr01419c>.
- (16) Roberts, A. S.; Pors, A.; Albrechtsen, O.; Bozhevolnyi, S. I. Subwavelength Plasmonic

- Color Printing Protected for Ambient Use. *Nano Lett.* **2014**, *14* (2), 783–787.  
<https://doi.org/10.1021/nl404129n>.
- (17) Tan, S. J.; Zhang, L.; Zhu, D.; Goh, X. M.; Wang, Y. M.; Kumar, K.; Qiu, C.-W.; Yang, J. K. W. Plasmonic Color Palettes for Photorealistic Printing with Aluminum Nanostructures. *Nano Lett.* **2014**, *14* (7), 4023–4029.  
<https://doi.org/10.1021/nl501460x>.
- (18) Shrestha, V. R.; Park, C.-S.; Lee, S.-S. Enhancement of Color Saturation and Color Gamut Enabled by a Dual-Band Color Filter Exhibiting an Adjustable Spectral Response. *Opt. Express* **2014**, *22* (3), 3691. <https://doi.org/10.1364/OE.22.003691>.
- (19) Cheng, F.; Gao, J.; Luk, T. S.; Yang, X. Structural Color Printing Based on Plasmonic Metasurfaces of Perfect Light Absorption. *Sci. Rep.* **2015**, *5* (1), 11045.  
<https://doi.org/10.1038/srep11045>.
- (20) Hu, X. L.; Sun, L. B.; Zeng, B.; Wang, L. S.; Yu, Z. G.; Bai, S. A.; Yang, S. M.; Zhao, L. X.; Li, Q.; Qiu, M.; et al. Polarization-Independent Plasmonic Subtractive Color Filtering in Ultrathin Ag Nanodisks with High Transmission. *Appl. Opt.* **2016**, *55* (1), 148. <https://doi.org/10.1364/AO.55.000148>.
- (21) Hail, C. U.; Schnoering, G.; Damak, M.; Poulikakos, D.; Eghlidi, H. A Plasmonic Painter's Method of Color Mixing for a Continuous Red-Green-Blue (RGB) Palette. *ACS Nano* **2020**. <https://doi.org/10.1021/acsnano.9b07523>.
- (22) Ooms, M. D.; Jeyaram, Y.; Sinton, D. Disposable Plasmonics: Rapid and Inexpensive Large Area Patterning of Plasmonic Structures with CO<sub>2</sub> Laser Annealing. *Langmuir* **2015**, *31* (18), 5252–5258. <https://doi.org/10.1021/acs.langmuir.5b01092>.

- (23) Roberts, A. S.; Novikov, S. M.; Yang, Y.; Chen, Y.; Boroviks, S.; Beermann, J.; Mortensen, N. A.; Bozhevolnyi, S. I. Laser Writing of Bright Colors on Near-Percolation Plasmonic Reflector Arrays. *ACS Nano* **2018**, acsnano.8b07541. <https://doi.org/10.1021/acsnano.8b07541>.
- (24) Nyga, P.; Chowdhury, S. N.; Kudyshev, Z.; Thoreson, M. D.; Kildishev, A. V.; Shalaev, V. M.; Boltasseva, A. Laser-Induced Color Printing on Semicontinuous Silver Films: Red, Green and Blue. *Opt. Mater. Express* **2019**, 9 (3), 1528. <https://doi.org/10.1364/OME.9.001528>.
- (25) Kirkpatrick, S. Percolation and Conduction. *Rev. Mod. Phys.* **1973**, 45 (4), 574–588. <https://doi.org/10.1103/RevModPhys.45.574>.
- (26) Yagil, Y.; Gadenne, P.; Julien, C.; Deutscher, G. Optical Properties of Thin Semicontinuous Gold Films over a Wavelength Range of 2.5 to 500 Mm. *Phys. Rev. B* **1992**, 46 (4), 2503–2511. <https://doi.org/10.1103/PhysRevB.46.2503>.
- (27) Shalaev, V. M.; Botet, R.; Butenko, A. V. Localization of Collective Dipole Excitations on Fractals. *Phys. Rev. B. Condens. Matter* **1993**, 48 (9), 6662–6664.
- (28) Kreibig, U.; Vollmer, M. *Optical Properties of Metal Clusters*; Springer Series in Materials Science; Springer Berlin Heidelberg: Berlin, Heidelberg, 1995; Vol. 25. <https://doi.org/10.1007/978-3-662-09109-8>.
- (29) Shalaev, V. M. Electromagnetic Properties of Small-Particle Composites. *Phys. Rep.* **1996**, 272 (2–3), 61–137. [https://doi.org/10.1016/0370-1573\(95\)00076-3](https://doi.org/10.1016/0370-1573(95)00076-3).
- (30) Grésillon, S.; Aigouy, L.; Boccara, A. C.; Rivoal, J. C.; Quelin, X.; Desmarest, C.; Gadenne, P.; Shubin, V. A.; Sarychev, A. K.; Shalaev, V. M. Experimental Observation

- of Localized Optical Excitations in Random Metal-Dielectric Films. *Phys. Rev. Lett.* **1999**, 82 (22), 4520–4523. <https://doi.org/10.1103/PhysRevLett.82.4520>.
- (31) Sarychev, A. K.; Shubin, V. A.; Shalaev, V. M. Anderson Localization of Surface Plasmons and Nonlinear Optics of Metal-Dielectric Composites. *Phys. Rev. B* **1999**, 60 (24), 16389–16408. <https://doi.org/10.1103/PhysRevB.60.16389>.
- (32) Shalaev, V. M. *Optical Properties of Nanostructured Random Media*; Springer, 2001.
- (33) Rautian, S. G.; Safonov, V. P.; Chubakov, P. A.; Shalaev, V. M.; Shtokman, M. I. Giant Parametric Light Scattering by Silver Clusters. *PZETF* **1988**, 47, 200–203.
- (34) Bragg, W. D.; Markel, V. A.; Kim, W.-T.; Banerjee, K.; Young, M. R.; Zhu, J. G.; Armstrong, R. L.; Shalaev, V. M.; Ying, Z. C.; Danilova, Y. E.; et al. Near-Field Optical Study of Selective Photomodification of Fractal Aggregates. *J. Opt. Soc. Am. B* **2001**, 18 (5), 698. <https://doi.org/10.1364/josab.18.000698>.
- (35) Novikov, S. M.; Frydendahl, C.; Beermann, J.; Zenin, V. A.; Stenger, N.; Coello, V.; Mortensen, N. A.; Bozhevolnyi, S. I. White Light Generation and Anisotropic Damage in Gold Films near Percolation Threshold. *ACS Photonics* **2017**, 4 (5), 1207–1215. <https://doi.org/10.1021/acsp Photonics.7b00107>.
- (36) Karpov, A. V.; Popov, A. K.; Rautian, S. G.; Safonov, V. P.; Slabko, V. V.; Shalaev, V. M.; Shtokman, M. I. Observation of a Wavelength- and Polarization-Selective Photomodification of Silver Clusters. *JETP Lett.* **1988**, 48 (10), 571.
- (37) Bragg, W. D.; Safonov, V. P.; Kim, W.; Banerjee, K.; Young, M. R.; Zhu, J. G.; Ying, Z. C.; Armstrong, R. L.; Shalaev, V. M. Near-Field Optical Studies of Local Photomodification in Nanostructured Materials. *J. Microsc.* **1999**, 194 (2–3), 574–577.

<https://doi.org/10.1046/j.1365-2818.1999.00542.x>.

- (38) Nyga, P.; Thoreson, M. D.; de Silva, V.; Yuan, H.-K.; Drachev, V. P.; Shalaev, V. M. Infrared Filters Based on Photomodification of Semicontinuous Metal Films. In *Frontiers in Optics*; OSA: Washington, D.C., 2006; p FTuU3. <https://doi.org/10.1364/FIO.2006.FTuU3>.
- (39) Nyga, P.; Drachev, V. P.; Thoreson, M. D.; Shalaev, V. M. Mid-IR Plasmonics and Photomodification with Ag Films. *Appl. Phys. B* **2008**, *93* (1), 59–68. <https://doi.org/10.1007/s00340-008-3145-9>.
- (40) Chettiar, U. K.; Nyga, P.; Thoreson, M. D.; Kildishev, A. V.; Drachev, V. P.; Shalaev, V. M. FDTD Modeling of Realistic Semicontinuous Metal Films. *Appl. Phys. B* **2010**, *100* (1), 159–168. <https://doi.org/10.1007/s00340-010-3985-y>.
- (41) Markel, V. A.; Muratov, L. S.; Stockman, M. I.; George, T. F. Theory and Numerical Simulation of Optical Properties of Fractal Clusters. *Phys. Rev. B* **1991**, *43* (10), 8183–8195. <https://doi.org/10.1103/PhysRevB.43.8183>.
- (42) Safonov, V. P.; Shalaev, V. M.; Markel, V. A.; Danilova, Y. E.; Lepeshkin, N. N.; Kim, W.; Rautian, S. G.; Armstrong, R. L. Spectral Dependence of Selective Photomodification in Fractal Aggregates of Colloidal Particles. *Phys. Rev. Lett.* **1998**, *80* (5), 1102–1105. <https://doi.org/10.1103/PhysRevLett.80.1102>.
- (43) Genov, D. A.; Sarychev, A. K.; Shalaev, V. M. Metal-Dielectric Composite Filters with Controlled Spectral Windows of Transparency. *J. Nonlinear Opt. Phys. Mater.* **2003**, *12* (04), 419–440. <https://doi.org/10.1142/S0218863503001559>.
- (44) Berean, K. J.; Sivan, V.; Khodasevych, I.; Boes, A.; Della Gaspera, E.; Field, M. R.;

- Kalantar-Zadeh, K.; Mitchell, A.; Rosengarten, G. Laser-Induced Dewetting for Precise Local Generation of Au Nanostructures for Tunable Solar Absorption. *Adv. Opt. Mater.* **2016**, *4* (8), 1247–1254. <https://doi.org/10.1002/adom.201600166>.
- (45) Raza, S.; Lavieja, C.; Zhu, X.; Kristensen, A. Resonant Laser Printing of Bi-Material Metasurfaces: From Plasmonic to Photonic Optical Response. *Opt. Express* **2018**, *26* (16), 20203. <https://doi.org/10.1364/oe.26.020203>.
- (46) Oh, H.; Lee, J.; Seo, M.; Baek, I. U.; Byun, J. Y.; Lee, M. Laser-Induced Dewetting of Metal Thin Films for Template-Free Plasmonic Color Printing. *ACS Appl. Mater. Interfaces* **2018**, *10* (44), 38368–38375. <https://doi.org/10.1021/acsami.8b13675>.
- (47) Mao, F.; Davis, A.; Tong, Q. C.; Luong, M. H.; Nguyen, C. T.; Ledoux-Rak, I.; Lai, N. D. Direct Laser Writing of Gold Nanostructures: Application to Data Storage and Color Nanoprinting. *Plasmonics* **2018**, *13* (6), 2285–2291. <https://doi.org/10.1007/s11468-018-0751-1>.
- (48) Cui, X.; Zhu, X.; Shao, L.; Wang, J.; Kristensen, A. Plasmonic Color Laser Printing inside Transparent Gold Nanodisk-Embedded Poly(Dimethylsiloxane) Matrices. *Adv. Opt. Mater.* **2020**, *8* (1), 1901605. <https://doi.org/10.1002/adom.201901605>.
- (49) Kuroiwa, Y.; Tatsuma, T. Laser Printing of Translucent Plasmonic Full-Color Images with Transmission-Scattering Dichroism of Silver Nanoparticles. *ACS Appl. Nano Mater.* **2020**, *acsanm.9b02560*. <https://doi.org/10.1021/acsanm.9b02560>.
- (50) Cui, X.; Zhu, X.; Shao, L.; Wang, J.; Kristensen, A. Plasmonic Color Laser Printing inside Transparent Gold Nanodisk-Embedded Poly(Dimethylsiloxane) Matrices. *Adv. Opt. Mater.* **2020**, *8* (1), 1901605. <https://doi.org/10.1002/adom.201901605>.

- (51) Zhu, X.; Vannahme, C.; Højlund-Nielsen, E.; Mortensen, N. A.; Kristensen, A. Plasmonic Colour Laser Printing. *Nat. Nanotechnol.* **2016**, *11* (4), 325–329. <https://doi.org/10.1038/nnano.2015.285>.
- (52) Pors, A.; Bozhevolnyi, S. I. Plasmonic Metasurfaces for Efficient Phase Control in Reflection. *Opt. Express* **2013**, *21* (22), 27438. <https://doi.org/10.1364/OE.21.027438>.
- (53) Chowdhury, S. N.; Nyga, P.; Kudyshev, Z.; Kildishev, A. V.; Shalaev, V. M.; Boltasseva, A. Laser Color Printing on Semicontinuous Silver Films. In *Optics InfoBase Conference Papers*; 2019; Vol. Part F127-. [https://doi.org/10.1364/CLEO\\_AT.2019.JW2A.55](https://doi.org/10.1364/CLEO_AT.2019.JW2A.55).
- (54) Chowdhury, S. N. .; Nyga, P.; Kudyshev, Z.; Garcia, E.; Kildishev, A. V.; Shalaev, V. M.; Boltasseva, A. Non-Fading Plasmonic Color Printing on Semicontinuous Metal Films with Protective Atomic Layer Deposition. In *Conference on Lasers and Electro-Optics*; Optical Society of America: San Francisco, 2020; p SF2R.2.
- (55) Nyga, P.; Kildishev, A. V.; Chowdhury, S. N.; Boltasseva, A.; Kudyshev, Z.; Shalaev, V. M. Optical Device, Method of Using the Same, and Method of Making the Same (Patent Pending).
- (56) Wang, X.; Santschi, C.; Martin, O. J. F. Strong Improvement of Long-Term Chemical and Thermal Stability of Plasmonic Silver Nanoantennas and Films. *Small* **2017**, *13* (28), 1700044. <https://doi.org/10.1002/sml.201700044>.
- (57) Groeneveld, R. H. M.; Sprik, R.; Lagendijk, A. Femtosecond Spectroscopy of Electron-Electron and Electron-Phonon Energy Relaxation in Ag and Au. *Phys. Rev. B* **1995**, *51* (17), 11433–11445. <https://doi.org/10.1103/PhysRevB.51.11433>.

- (58) Nanophotonic FDTD Simulation Software - Lumerical FDTD Solutions  
<https://www.lumerical.com/products/fdtd-solutions/>.
- (59) Thoreson, M. D.; Fang, J.; Kildishev, A. V.; Prokopenko, L. J.; Nyga, P.; Chettiar, U. K.; Shalaev, V. M.; Drachev, V. P. Fabrication and Realistic Modeling of Three-Dimensional Metal-Dielectric Composites. *J. Nanophotonics* **2011**, 5 (1), 051513.  
<https://doi.org/10.1117/1.3590208>.
- (60) George, S. M. Atomic Layer Deposition: An Overview. *Chem. Rev.* **2010**, 110 (1), 111–131. <https://doi.org/10.1021/cr900056b>.
- (61) Albrecht, G.; Kaiser, S.; Giessen, H.; Hentschel, M. Refractory Plasmonics without Refractory Materials. *Nano Lett.* **2017**, 17 (10), 6402–6408.  
<https://doi.org/10.1021/acs.nanolett.7b03303>.
- (62) Groner, M. D.; Fabreguette, F. H.; Elam, J. W.; George, S. M. Low-Temperature Al<sub>2</sub>O<sub>3</sub> Atomic Layer Deposition. **2004**. <https://doi.org/10.1021/CM0304546>.
- (63) Jaffé, A. *CG Jung, Word and Image*; Princeton University Press, 1979.
- (64) Origin: Data Analysis and Graphing Software  
<https://www.originlab.com/index.aspx?go=Products/Origin>.
- (65) Wyszecki, G.; Stiles, W. S. *Color Science: Concepts and Methods, Quantitative Data and Formulae*, 2nd ed.; Wiley: New York, 1982.